IEEE Access
Multidisciplinary ⋮ Rapid Review ⋮ Open Access Journal

Received February 13, 2019, accepted February 28, 2019, date of publication March 5, 2019, date of current version April 1, 2019.

Digital Object Identifier 10.1109/ACCESS.2019.2903147

A Band-Pass Filter Based on the Spoof Surface Plasmon Polaritons and CPW-Based Coupling Structure

JUN WANG[1,2], (Student Member, IEEE), LEI ZHAO[2,3], (Senior Member, IEEE), AND ZHANG-CHENG HAO[1,4], (Senior Member, IEEE)

[1]State Key Laboratory of Millimeter-Waves, School of Information Science and Engineering, Southeast University, Nanjing 211189, China
[2]Center for Computational Science and Engineering, School of Mathematics and Statistics, Jiangsu Normal University, Xuzhou 221116, China
[3]School of Information and Control Engineering, China University of Mining and Technology, Xuzhou 221116, China
[4]Purple Mountain Laboratories, Nanjing 211111, China

Corresponding authors: Lei Zhao (leizhao@cumt.edu.cn) and Zhang-Cheng Hao (zchao@seu.edu.cn)

This work was supported in part by the National Science Foundation of China under Grant 61771226 and Grant 61372057, in part by the Natural Science Foundation of the Jiangsu Higher Education Institutions of China under Grant 18KJA110001, and in part by the Natural Science Foundation of the Xuzhou of China under GrantKC18003.

ABSTRACT In this paper, a band-pass filter based on the spoof surface plasmon polaritons (SSPPs) and coplanar waveguide (CPW)-based coupling structure is proposed. The design concept of the proposed band-pass filter is to use the SSPP structure and CPW-based coupling structure for controlling the high cut-off frequency and filtering the low-frequency wave, respectively, which means that the low and high cut-off frequencies of the band-pass filter can be independently controlled. The physical mechanism of the proposed band-pass filter is explained with the aid of dispersion curves, electric field distributions, and equivalent circuits. Moreover, parametric studies are conducted to analyze the effects of the key parameters on the controllable performance of the band-pass filter, which is useful for practical designs. Furthermore, in order to improve the high-frequency performance, the split ring resonators are added to the structure. The simulation results show that the proposed band-pass filter achieves a bandwidth (for $|S_{11}| < -10$ dB and $|S_{21}| > -1.6$ dB) of 35.9% (7.31–10.51 GHz). The experimental results validate the proposed concept and measured results are in a good agreement with simulated ones, which indicate that the proposed band-pass filter is believed to be significantly promising for further developing plasmonic functional devices at microwave frequencies.

INDEX TERMS Band-pass filter, CPW-based coupling structure, split ring resonators, spoof surface plasmon polaritons.

I. INTRODUCTION

Spoof surface plasmon polaritons (SSPPs) have been widely utilized in the microwave applications, such as circulator [1], various antennas [2]–[4], and surface plasmonic filters [5]–[7]. Compared with the traditional microwave devices, the SSPP structures have the following special advantages, such as confining the microwave field in sub-wavelength size, resisting electromagnetic (EM) interference, and wide bandwidth. Additionally, it can break through the diffraction limit to realize the miniaturization of the microwave devices. Therefore, a band-pass filter based on the SSPPs can be a good candidate for future microwave communications.

Recently, the band-pass filters based on the microstrip line [8]–[13], substrate-integrated waveguide (SIW) [14]–[18], lumped element [19], [20], and SSPP geometries [7] [21]–[24] have been reported. The microstrip band-pass filters were basically designed using the series or parallel connection of the microstrip line structure [8], [9], microstrip fed [10], and slotted ground structure [11]–[13]. Moreover, some SIW designs were also proposed in [14]–[18] to realize low cost, high quality factor, and easy fabrication band-pass performance. Nevertheless, most of them only realize a controllable frequency or bandwidth performance, which is difficult to achieve the fully controllable performance

The associate editor coordinating the review of this manuscript and approving it for publication was Yingsong Li.

(the independent controllability of low and high cut-off frequencies). In order to achieve fully controllable band-pass filter, the designs based on the lumped elements were proposed to realize independent controllability of frequencies [19], [20]. However, these designs are electronically controllable and it is not a planar structure and the fabrication cost is high. Therefore, designing a planar mechanically controllable band-pass filter with the independent controllability of low and high cut-off frequencies and low cost is technically very challenging. Accordingly, the SSPP-based structures are the suitable candidate for high cut-off frequency controlling, due to its advantages of high cut-off frequency can be easily controlled by optimizing the geometrical parameters [7] [21]–[24]. In addition, some CPW-based or microstrip-based coupling structures [25]–[28] maybe a good candidate to control the low cut-off frequency after a modification. However, how to combine the modified CPW-based coupling structure with the SSPPs is a difficult problem.

In this paper, we propose a mechanically controllable band-pass filter, which are composed of three parts: 1) SSPP-based waveguide low-pass filter with periodic holes etched on the standard 50-Ω CPW, which controls the high cut-off frequency [29]; 2) a CPW-based coupling structure is used for controlling the low frequency band; 3) the split ring resonators (SRRs) [30]–[34] are added for enhancing the high frequency performance. In addition, the physical mechanisms are carefully investigated for better understanding based on the dispersion curves, electric field distributions, and equivalent circuits. The characteristic of our proposed band-pass filter is verified through both numerical simulations and experimental measurements. The proposed design has the following features: 1) the low and high cut-off frequencies of the band-pass structure can be independently controlled by changing different parameters, respectively; 2) the equivalent circuit model is proposed to explain the proposed band-pass filter; 3) the pass band has a good transmission efficiency; 4) simple, flexible, and low fabrication cost design makes it easy for microwave applications.

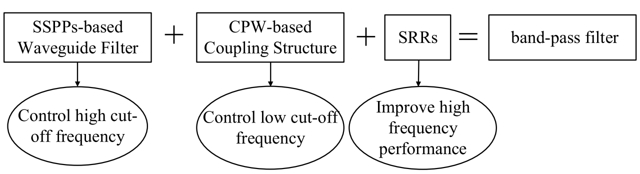

FIGURE 1. Design concept of the proposed band-pass filter.

II. DESIGN CONCEPT AND CONFIGURATION

The design idea of the proposed band-pass filter is sketched in Fig. 1, which is a common SSPPs with the CPW-based coupling structure and the split ring resonators (SRRs) to realize a good band-pass performance. The SSPPs is used to control the high cut-off frequency by changing the unit cell length and the CPW-based coupling structure controls the low cut-off frequency by changing the bottom metal length. In addition, the SRRs are added in the structure to improve the high frequency performance of the proposed band-pass filter.

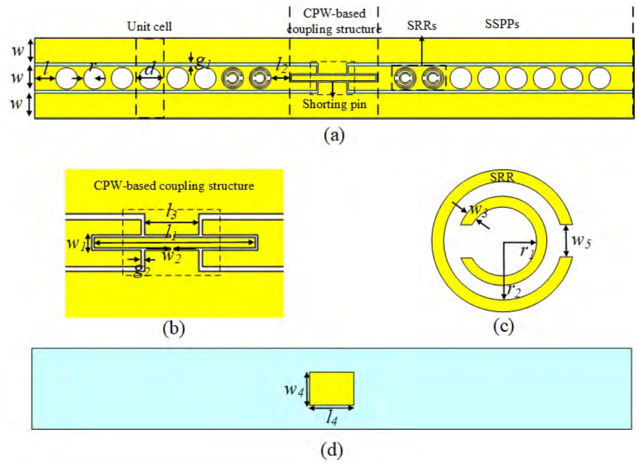

FIGURE 2. Configuration of the proposed band-pass filter. (a) Top view. (b) CPW-based coupling structure. (c) SRR. (d) Bottom view.

Based on the above design concept, the configuration of the proposed band-pass filter is presented in Fig. 2. The structure is printed on the 0.5 mm thick Taconic RF-35 substrate (relative permittivity $\varepsilon_r = 3.5$, loss tangent $\tan\delta = 0.0018$). The SSPPs is composed of a 50-Ω CPW transmission line with periodic holes etched on the middle line. The designed parameters of the width and gap of CPW striplines are denoted by w and g_1, respectively. The length of CPW feeding part is marked as l. Likewise, the periodic holes have a radius of r and the length of a unit cell is marked as d, as shown in the dashed box. Moreover, the length and width of the middle line of the CPW-based coupling structure are defined as l_1 and w_1, respectively. The length between the SRRs and the middle line of the CPW-based coupling structure is marked as l_2. The gap of the CPW-based coupling structure is g_2. Additionally, the width of the shorting pins and the length of the connected ground of CPW are denoted by w_2 and l_3, respectively. The length and width of the metal of the CPW-based coupling structure on the bottom of the substrate are marked as l_4 and w_4. Furthermore, the dimensions of the SRR are presented in Fig. 2(c), the radii of the inner and outer are r_1 and r_2, respectively. In addition, the thickness of the split ring is w_3 and the width of the open space of the split ring is w_5.

III. DESIGN CONSIDERATIONS

The proposed band-pass filter combines the SSPP-based waveguide filter [29] and a CPW-based coupling structure, while adding the SRRs to improve the high frequency performance. The SSPP-based waveguide filter can support the SSPPs modes on the CPW surface and converts the quasi-TEM wave on the CPW to SSPPs wave efficiently by using the periodic holes etched on the CPW. Meanwhile, the length of the unit cell (d) controls the high cut-off frequency, which decreases with the d increases. Moreover, the CPW-based coupling structure is employed as a capacitor to filter the low frequency wave, which controls the low cut-off frequency by changing the length of metal (l_4) printed on the bottom layer of the substrate. Furthermore, the band-stop SRRs are added in the structure to improve the high frequency performance.

A. MODE CONVERSION FROM Quasi-TEM WAVE TO TM WAVE

The SSPP-based waveguide filter is used to control the high frequency performance, which is a common CPW line etched with periodic holes [29]. The unit cell of the waveguide is presented in the dashed box, as shown in Fig. 2(a). The dispersion curves and the electric field distributions are simulated using the full-wave electromagnetic (EM) simulation software CST. The dispersion curves for the fundamental mode of the SSPP-based waveguide filter with different unit cell length (d) are plotted in Fig. 3(a). It is seen that the dispersion curves deviate from the CPW line significantly with the increased unit cell length (d) when r is fixed as 2.88 mm. Additionally, it is clear from Fig. 3(b) that the hole radius has little influence on the dispersion curves when d is fixed as 7.5 mm, except that if the diameter of the hole very close to the width of the CPW line, the dispersion curves will deviate dramatically. Generally, the wave momentums of the fundamental mode are gradually deviating from the CPW line and the cut-off frequency of the SSPP-based waveguide filter decreases as the unit cell length (d) and hole radius (r) raises.

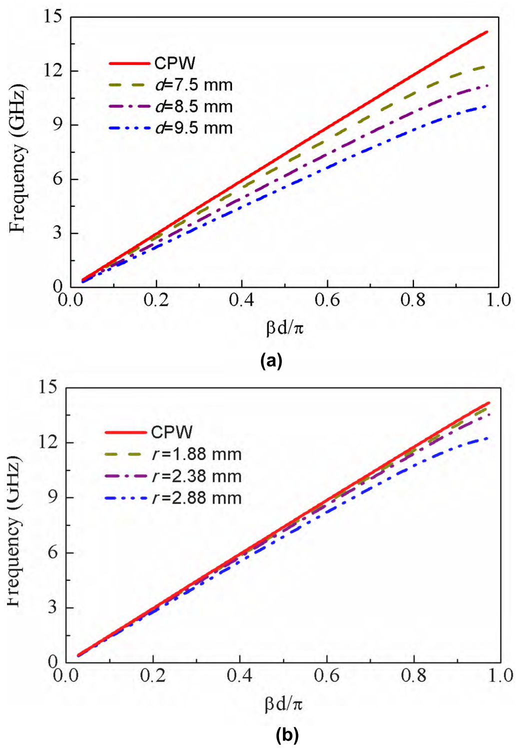

FIGURE 3. (a) Simulated dispersion curves for the fundamental mode of the SSPP-based waveguide filter with different unit cell length and (b) with different holes radii.

In order to further show the excellent field confinement and good propagation property of the SSPP-based waveguide filter, the simulated electric field distribution on the x-y plane and the magnitudes of energy flows on cross sections at 9 GHz when $d = 7.5$ mm are plotted in Fig. 4(a) and (b), respectively. Fig. 4(c) shows the power flow at y-z planes cutting the circular hole of the SSPP-based waveguide filter at 9 GHz. The color scale ranges from red (highest intensity) to dark blue (lowest intensity), and the black line denotes the modal size of the proposed SSPP mode, which represents most of the integrated energy flow are limited in 0.27 λ (λ is the wavelength at 9 GHz). It is seen that from Fig. 4, the EM fields are highly localized on the adjacent CPW lines and adjacent holes and are tightly confined in the deep subwavelength scale around the waveguide and the SPP wave propagates, which indicate that most of EM energy is highly localized within a small region in the SSPP-based waveguide filter. Hence, the CPW-based waveguide structure can support the modes of SSPPs propagation on the CPW surface and convert the quasi-TEM wave to SSPP (TM) wave efficiently.

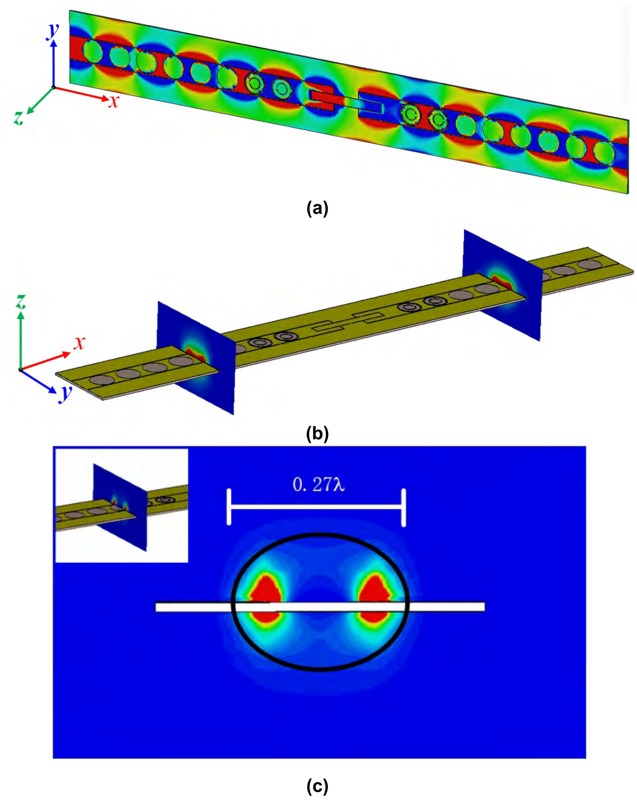

FIGURE 4. (a) The electric field distribution on the x-y plane at 9 GHz when $d = 7.5$ mm. (b) The magnitudes of electric field flow on cross sections of the SSPP-based waveguide filter at two different locations at 9 GHz when $d = 7.5$ mm. (c) Power flow at y-z planes cutting the circular hole of the SSPP-based waveguide filter at 9 GHz.

B. EQUIVALENT CIRCUIT OF THE PROPOSED BAND-PASS FILTER

To further physically explain the whole structure behavior, a simplified LC equivalent circuits (neglecting R as its value will be negligibly small in case of metals) of the CPW feeding part, unit cell, SRR, and CPW-based coupling structure are shown in Fig. 5. In the equivalent circuits, each conducting

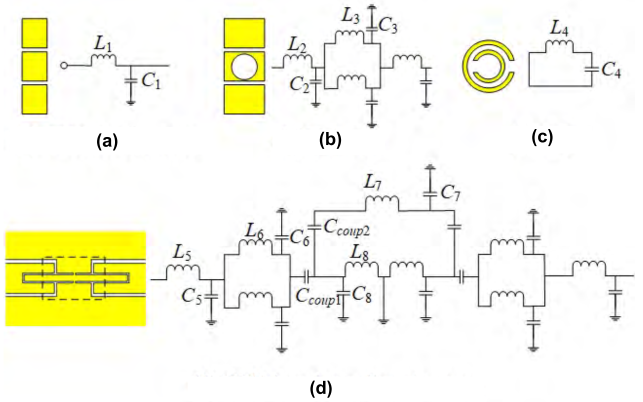

FIGURE 5. Simplified equivalent circuits of the (a) CPW feeding part, (b) unit cell, (c) SRR, and (d) CPW-based coupling structure.

line in the design can be modeled as an inductance while any pair of parallel conducting edges is represented by some capacitance values, and the values of L and C represent per-unit-length values. The values of L_1 and C_1 of CPW feeding part can be derived from [35] and [36] and can be expressed as:

$$L_1 = Z_0 \frac{\sqrt{\varepsilon_{re}}}{c_0}, \quad (1)$$

$$C_1 = \frac{L_1}{Z_0^2}. \quad (2)$$

where Z_0 is the characteristic impedance of the CPW feeding part, ε_{re} is the effective dielectric constant, and c_0 is the velocity of light in frees pace. Moreover, the values of equivalent L_4 and C_4 of SRR may be calculated as [34]:

$$L_4 = \mu_0 R_m \left[\ln\left(\frac{2.8 R_m}{w_3}\right) - 1.75 \right], \quad (3)$$

$$C_4 = \frac{\pi R_m}{2} C_p. \quad (4)$$

in which μ_0 is the permeability of free space, R_m is the mean radius of SRR ($R_m = r_2 - (r_2 - r_1 - w_3)/2$), and C_p is the capacitance per-unit-length along the slot between the rings, which can be obtained from [35].

Based on the above equivalent circuits, a simplified equivalent circuit model for the whole system is synthesized by merging the L and C of the adjacent unit cells, as shown in Fig. 6, which utilizes the equivalent circuits of the CPW feeding part, unit cell, and simplified CPW-based coupling structure cascaded each other and the SRRs paralleled to the last two unit cells. This schematic can be used to understand the performance of the system in circuital terms, and as a useful tool for future designs. According to formulas (1)-(3) and using the advanced design system (ADS) software to optimize the values, the values of the equivalent circuit are empirically calculated as: $L_1' = 0.353$ nH, $L_2' = 0.419$ nH, $L_3' = 0.336$ nH, $L_4' = 3.98$ nH, $L_5' = 0.662$ nH, $L_6' = 6.31$ nH, $L_7' = 0.009$ nH, $L_8' = 0.293$ nH, $C_1' = 0.174$ pF, $C_2' = 0.001$ pF, $C_3' = 0.165$ pF, $C_4' = 0.058$ pF, $C_5' = 0.326$ pF, $C_6' = 0.0193$ pF, $C_7' = 2.83$ pF, $C_8' = 0.242$ pF, $C_s = 0.917$ pF, $C_{coup1}' = 0.1$ pF, $C_{coup2}' = 1.17$ pF.

C. BAND-PASS FILTER PERFORMANCE

Following the geometrical description and physical mechanism explained above, the band-pass filter performance is now investigated. The full-wave simulation results are demonstrated together with the scattering parameters of the corresponding simplified equivalent circuit model, as shown in Fig. 7. It is seen that the simulation results of the equivalent circuit model present the similar trend with the full-wave simulation results, which validate the proposed design exhibits the expected behavior. Moreover, it should be noted that the differences between circuit model and physical model responses at lower and higher frequencies are caused by the simplified circuit model of CPW-based coupling structure and unit cell, which ignore a small amount of coupling between the structures.

To improve the high frequency performance of the proposed band-pass filter, four SRR elements are added in the structure. The simulated results with and without SRRs are presented in Fig. 8, which show that the SRRs can cancel the high frequency resonance about at 11.7 GHz and have no influence on the low frequency performance. Additionally, simulation results show that the proposed band-pass filter can achieve a bandwidth (for $|S_{11}| < -10$ dB and $|S_{21}| > -1.6$ dB) of 35.9% (7.31–10.51 GHz). Moreover, it should be mentioned that a slender shorting pin is used in the structure (as shown in Fig. 2) to connect the middle coupling metal line and the ground, which plays an important role on the whole design. The band-pass filter will not work if the shorting pin is removed, and as well as in the corresponding equivalent circuit model which means that the grounding lumped-element between two inductors (L_8') is necessary for the whole circuit.

D. PARAMETRIC STUDIES ON THE KEY PARAMETERS

In order to study the controllability of the proposed band-pass filter, parametric studies on the key parameters are conducted to analyze the effects of these parameters on performance, which are useful to the practical design of a SSPP-based band-pass filter. The low and high cut-off frequencies of the proposed band-pass filter are mainly controlled by two key parameters, respectively. The length of metal of the CPW-based coupling structure printed on the bottom substrate (l_4) is applied to control the low cut-off frequency, which decreases with the l_4 increases. Meanwhile, the length of unit cell (d) plays an important role on the high cut-off frequency controlling, which decreases with the d increases.

Fig. 9 shows the simulated transmission ($|S_{21}|$) and reflection ($|S_{11}|$) coefficients of the proposed band-pass filter with the SRR and l_4 changes from 8 mm to 12 mm with the step 1 mm. It is obvious that the parameter l_4 can control the low cut-off frequency significantly, which decreases with the parameter raises. Fig. 10 shows the effects of the unit cell d on the performance of the high cut-off frequency. It is seen that the high cut-off frequency decreases with the unit cell d raises and has a good agreement with the simulated dispersion curves (as shown in Fig. 3(a)). It should be noted

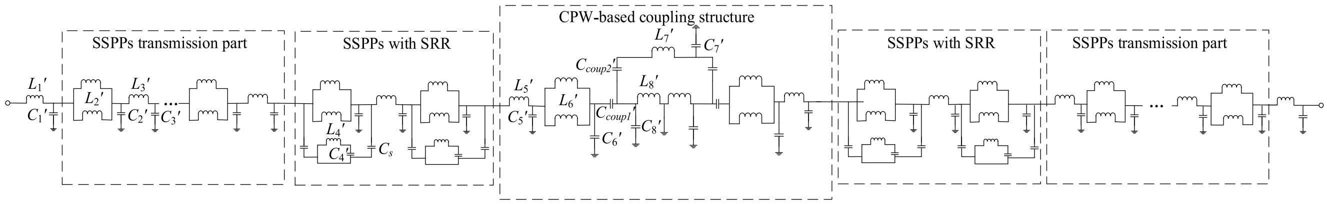

FIGURE 6. Simplified equivalent circuit of the whole structure.

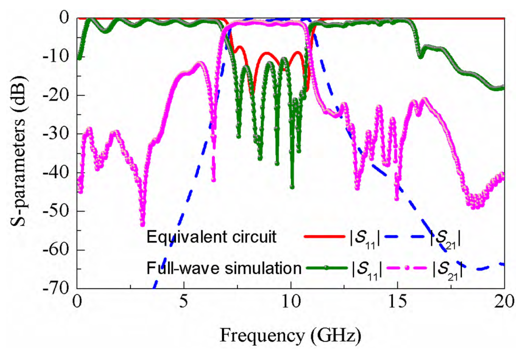

FIGURE 7. Simulated S-parameters of the proposed band-pass filter and equivalent circuit model.

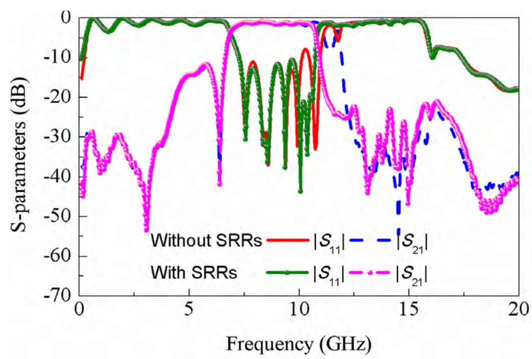

FIGURE 8. Simulated S-parameters of the proposed band-pass filter with and without SRRs.

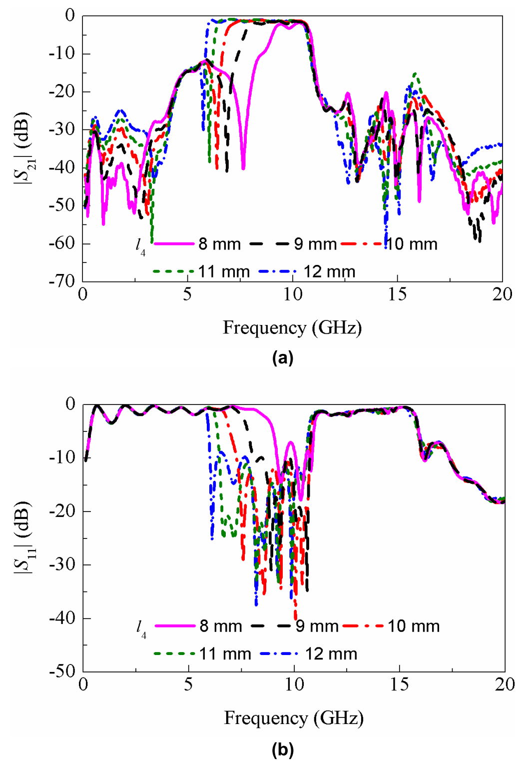

FIGURE 9. Simulated transmission ($|S_{21}|$) coefficients (a) and reflection ($|S_{11}|$) coefficients (b) of the proposed band-pass filter with SRR and l4 changes from 8 mm to 12 mm with the step 1 mm.

the parametric study on d does not include the SRRs, due to the SRRs are only used for the performance enhancement of the high frequency and some $|S_{11}|$ points are a little higher than -10 dB, which can be cancelled by the fine adjustment of the structure. Generally, the low and high cut-off frequencies decrease as the length of bottom metal (l_4) and unit cell (d) increase. Converting to the LC equivalent circuit, the corresponding values of L and C in the equivalent circuit will raise, leading to the frequencies bring down.

From the parametric studies above, the proposed band-pass filter shows a good controllability of the low and high cut-off frequencies by independently tuning different parameters l_4 and d, respectively, which can be used in many applications for microwave and RF engineering.

IV. EXPERIMENTAL VERIFICATION

A prototype is fabricated to characterize the performance of the proposed filter, as shown in Fig. 11. The prototype is fabricated using the standard printed circuit board technologies. The substrate used is the 0.5 mm Taconic RF-35 substrate with $\varepsilon_r = 3.5$, loss tangent $\tan\delta = 0.0018$, and the metallic strips have a thickness of 0.035 mm, which is much greater than the skin depth of copper, and therefore copper is considered to be a perfect electrical conductor. The fabricated band-pass filter physical dimensions are as follows: $l = 3.57$ mm, $l_1 = 19.2$ mm, $l_2 = 5.17$ mm, $l_3 = 6.6$ mm, $l_4 = 10$ mm, $w = 6$ mm, $w_1 = 2.4$ mm, $w_2 = 0.2$ mm, $w_3 = 0.2$ mm, $w_4 = 6.8$ mm, $w_5 = 0.6$ mm, $r = 2.88$ mm, $r_1 = 1.3$ mm, $r_2 = 2.5$ mm, $g_1 = 0.2$ mm, $g_2 = 0.1$ mm, and $d = 7.5$ mm.

Fig. 12 presents the simulated and measured results of the proposed band-pass filter. It is seen that the measured results have a good agreement with the simulated ones. The simulated bandwidth (for $|S_{11}| < -10$ dB and $|S_{21}| > -1.6$ dB) is from 7.31 GHz to 10.51 GHz and the measured return loss is a little greater than the simulated one at high frequency, which is maybe caused by the SMA soldering and the fabricated tolerances. As expected, the fabricated

TABLE 1. Performance comparison of existing controllable band-pass filter.

Ref.	Design technique (Mechanically or electronically)	Minimum insertion loss (dB)	Controllability of bandwidth or center frequency	Controllability of the low frequency independently	Controllability of the high frequency independently	Cost
[10]	Microstrip fed (Mechanically)	1	Center frequency	No	No	high
[11]	Microstrip–CPW (Mechanically)	0.1	Bandwidth and center frequency	No	Yes	low
[12]	Microstrip slotline (Mechanically)	0.5	bandwidth	No	No	low
[17]	SIW (Mechanically)	1.16	Center frequency	No	No	low
[18]	SIW (Mechanically)	1.3	Center frequency	No	No	low
[19]	Lumped elements (Electronically)	0.75	Bandwidth and center frequency	Yes	Yes	high
[20]	Lumped elements (Electronically)	1	Bandwidth and center frequency	Yes	Yes	high
This work	SSPPs and CPW-based coupling structure (Mechanically)	0.83	Bandwidth and center frequency	Yes	Yes	low

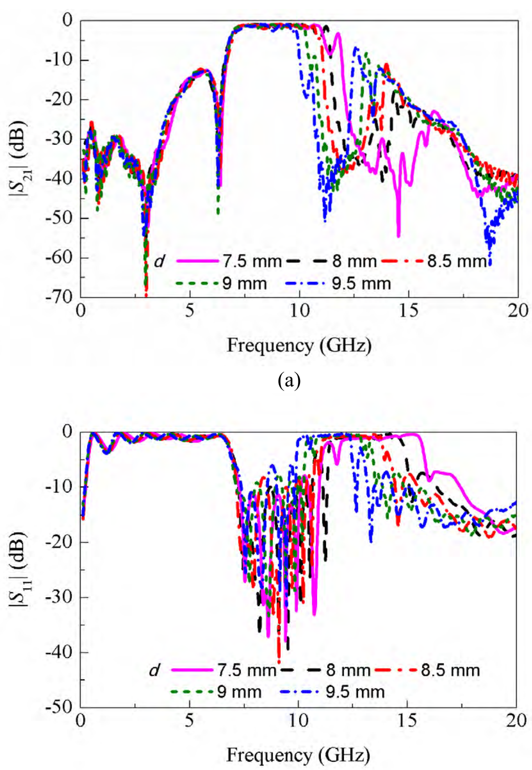

FIGURE 10. Simulated transmission ($|S_{21}|$) coefficients (a) and reflection ($|S_{11}|$) coefficients (b) of the proposed band-pass filter without the SRRs and d changes from 7.5 mm to 9.5 mm with the step 0.5 mm.

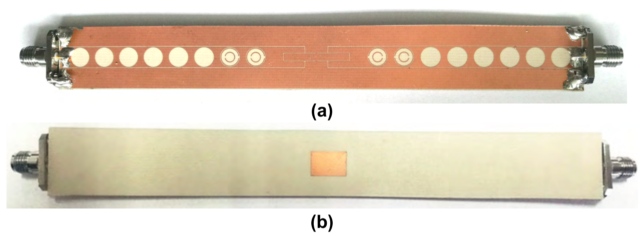

FIGURE 11. Photograph of the fabricated band-pass filter. (a) Top view; (b) Bottom view.

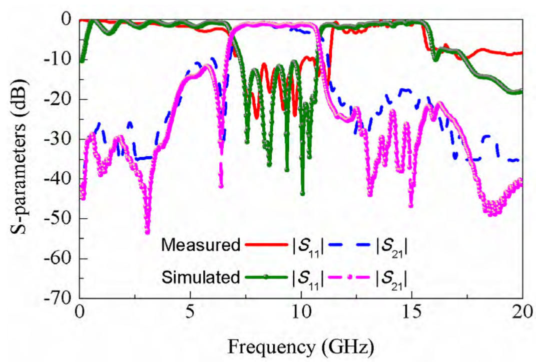

FIGURE 12. Measured and simulated S-parameters of the proposed band-pass filter.

structure and measured results validate the proposed concept and hold the promise to realize a good band-pass performance at the microwave frequency band.

Table 1 summarizes the performance comparison of existing controllable band-pass filters. It is seen that the traditional mechanically controllable microstrip filters in [10]–[12] retain much higher insertion loss than others and the SIW structures were also designed to achieve the mechanically controllable performance [17], [18]. However, most of the microstrip and SIW designs were difficult to design a mechanically fully controllable band-pass filter with the low and high cut-off frequencies can be controlled independently. Accordingly, the electronically lumped element band-pass filters were designed for microwave applications [19], [20]. Nevertheless, they are not planar structures and the fabrication cost is expensive. Therefore, compared to other band-pass filters, our proposed mechanically band-pass filter based on the SSPPs and CPW-based coupling structure exhibits the good advantages on the controllability of the frequency. In addition, our proposed band-pass is easy to fabricate with low cost and maybe has a great potential for microwave applications.

V. CONCLUSION

In this paper, a controllable band-pass filter based on the SSPPs and CPW-based coupling structure is proposed. The proposed concept and design are theoretically investigated using the dispersion curves, electric field distributions, and equivalent circuits. The low and high cut-off frequencies can be independently tuned by the related parameters. A prototype of the proposed filter has been fabricated, and the measured results are in good agreement with the simulated ones, which validates the proposed design concept. The proposed band-pass filter features some advantages compared to the reported structures, which makes it to be very useful for a wide variety of microwave applications.

REFERENCES

[1] T. Qiu, J. Wang, Y. Li, and S. Qu, "Circulator based on spoof surface plasmon polaritons," *IEEE Antennas Wireless Propag. Lett.*, vol. 16, pp. 821–824, 2016.

[2] A. Kianinejad, Z. N. Chen, L. Zhang, W. Liu, and C.-W. Qiu, "Spoof plasmon-based slow-wave excitation of dielectric resonator antennas," *IEEE Trans. Antennas Propag.*, vol. 64, no. 6, pp. 2094–2099, Jun. 2016.

[3] Y. J. Han *et al.*, "Multibeam antennas based on spoof surface plasmon polaritons mode coupling," *IEEE Trans. Antennas Propag.*, vol. 65, no. 3, pp. 1187–1192, Mar. 2017.

[4] Q. Zhang, Q. Zhang, and Y. Chen, "Spoof surface plasmon polariton leaky-Wave antennas using periodically loaded patches above PEC and AMC ground planes," *IEEE Antennas Wireless Propag. Lett.*, vol. 16, pp. 3014–3017, 2017.

[5] X. Zhang, L. Shen, and L. Ran, "Low-frequency surface plasmon polaritons propagating along a metal film with periodic cut-through slits in symmetric or asymmetric environments," *J. Appl. Phys.*, vol. 105, no. 1, Jan. 2009, Art. no. 013704.

[6] T. Jiang, L. Shen, X. Zhang, and L. Ran, "High-order modes of spoof surface plasmon polaritons on eriodically corrugated metal surfaces," *Prog. Electromagn. Res. M*, vol. 8, pp. 91–102, 2009.

[7] Y. J. Guo, K. D. Xu, Y. Liu, and X. Tang, "Novel surface plasmon polariton waveguides with enhanced field confinement for microwave-frequency ultra-wideband bandpass filters," *IEEE Access*, vol. 6, pp. 10249–10256, 2018.

[8] C.-W. Tang and M.-G. Chen, "A microstrip ultra-wideband bandpass filter with cascaded broadband bandpass and bandstop filters," *IEEE Trans. Microw. Theory Techn.*, vol. 55, no. 11, pp. 2412–2418, Nov. 2007.

[9] S.-W. Lan, M.-H. Weng, C.-Y. Hung, and S.-J. Chang, "Design of a compact ultra-wideband bandpass filter with an extremely broad stopband region," *IEEE Microw. Wireless Compon. Lett.*, vol. 26, no. 6, pp. 392–394, Jun. 2016.

[10] S. Kurudere and V. B. Ertürk, "Novel microstrip fed mechanically tunable combline cavity filter," *IEEE Microw. Wireless Compon. Lett.*, vol. 23, no. 11, pp. 578–580, Nov. 2013.

[11] T.-N. Kuo, S.-C. Lin, and C. H. Chen, "Compact ultra-wideband bandpass filters using composite microstrip–coplanar-waveguide structure," *IEEE Trans. Microw. Theory Techn.*, vol. 54, no. 10, pp. 3772–3778, Oct. 2006.

[12] D. Chen, H. Bu, L. Zhu, and C. Cheng, "A differential-mode wideband bandpass filter on slotline multi-mode resonator with controllable bandwidth," *IEEE Microw. Wireless Compon. Lett.*, vol. 25, no. 1, pp. 28–30, Jan. 2015.

[13] D. Chen, L. Zhu, H. Bu, and C. Cheng, "A wideband balun filter on a triple-mode slotline resonator with controllable bandwidth," *IEEE Microw. Wireless Compon. Lett.*, vol. 27, no. 6, pp. 569–571, Jun. 2017.

[14] C. Zhao, C. Fumeaux, and C.-C. Lim, "Folded substrate-integrated waveguide band-pass post filter," *IEEE Microw. Wireless Compon. Lett.*, vol. 27, no. 1, pp. 22–24, Jan. 2017.

[15] W. Lei, W. Che, K. Deng, and S. Dong, "Narrow-slot bandpass filter based on folded substrate-integrated waveguide with wide out-of-band rejection," *Microw. Opt. Technol. Lett.*, vol. 50, no. 5, pp. 1155–1159, May 2008.

[16] T. Yang, P.-L. Chi, R. Xu, and W. Lin, "Folded substrate integrated waveguide based composite right/left-handed transmission line and its application to partial H-plane filters," *IEEE Trans. Microw. Theory Techn.*, vol. 61, no. 2, pp. 789–799, Feb. 2013.

[17] K. Zhou, C.-X. Zhou, and W. Wu, "Substrate-integrated waveguide dual-mode dual-band bandpass filters with widely controllable bandwidth ratios," *IEEE Trans. Microw. Theory Techn.*, vol. 65, no. 10, pp. 3801–3812, Oct. 2017.

[18] H. Zhang, W. Kang, and W. Wu, "Miniaturized dual-band SIW filters using E-shaped slotlines with controllable center frequencies," *IEEE Microw. Wireless Compon. Lett.*, vol. 28, no. 4, pp. 311–313, Apr. 2018.

[19] Z.-H. Chen and Q.-X. Chu, "Wideband fully tunable bandpass filter based on flexibly multi-mode tuning," *IEEE Microw. Wireless Compon. Lett.*, vol. 26, no. 10, pp. 789–791, Oct. 2016.

[20] H. C. Zhang, P. H. He, X. Gao, W. X. Tang, and T. J. Cui, "Passband reconfigurable spoof surface plasmon polaritons," *J. Phys., Condens. Matter*, vol. 30, no. 13, Apr. 2018, Art. no. 134004.

[21] Y. J. Zhou and B. J. Yang, "Planar spoof plasmonic ultra-wideband filter based on low-loss and compact terahertz waveguide corrugated with dumbbell grooves," *Appl. Opt.*, vol. 54, no. 14, pp. 4529–4533, May 2015.

[22] H. F. Ma, X. Shen, Q. Cheng, W. X. Jiang, and T. J. Cui, "Broadband and high-efficiency conversion from guided waves to spoof surface plasmon polaritons," *Laser Photon. Rev.*, vol. 8, no. 1, pp. 146–151, Jan. 2014.

[23] L. Zhao *et al.*, "A novel broadband band-pass filter based on spoof surface plasmon polaritons," *Sci. Rep.*, vol. 6, Oct. 2016, Art. no. 36069.

[24] W. Zhang, G. Zhu, L. Sun, and F. Lin, "Trapping of surface plasmon wave through gradient corrugated strip with underlayer ground and manipulating its propagation," *Appl. Phys. Lett.*, vol. 106, no. 2, Jan. 2015, Art. no. 021104.

[25] H. L. Hu, X. D. Huang, and C. H. Cheng, "Ultra-wideband bandpass filter using CPW-to-microstrip coupling structure," *Electron. Lett.*, vol. 42, no. 10, pp. 586–587, May 2006.

[26] J.-W. Baik, T.-H. Lee, and Y.-S. Kim, "UWB bandpass filter using microstrip-to-CPW transition with broadband balun," *IEEE Microw. Wireless Compon. Lett.*, vol. 17, no. 12, pp. 846–848, Dec. 2007.

[27] L. Zhu and W. Menzel, "Broad-band microstrip-to-CPW transition via frequency-dependent electromagnetic coupling," *IEEE Trans. Microw. Theory Techn.*, vol. 52, no. 5, pp. 1517–1522, May 2004.

[28] A. Abbosh, S. Ibrahim, and M. Karim, "Ultra-wideband crossover using microstrip-to-coplanar waveguide transitions," *IEEE Microw. Wireless Compon. Lett.*, vol. 22, no. 10, pp. 500–502, Oct. 2012.

[29] J. Wang, L. Zhao, Z.-C. Hao, and T. J. Cui, "An ultra-thin coplanar waveguide filter based on the spoof surface plasmon polaritons," *Appl. Phys. Lett.*, vol. 113, no. 7, Aug. 2018, Art. no. 071101.

[30] J. D. Baena *et al.*, "Equivalent-circuit models for split-ring resonators and complementary split-ring resonators coupled to planar transmission lines," *IEEE Trans. Microw. Theory Techn.*, vol. 53, no. 4, pp. 1451–1461, Apr. 2005.

[31] C. Feng, T. Shi, and L. Wang, "Novel broadband bow-tie antenna based on complementary split-ring resonators enhanced substrate-integrated waveguide," *IEEE Access*, vol. 7, pp. 12397–12404, 2019.

[32] S. Zuffanelli, G. Zamora, P. Aguilàă, F. Paredes, F. Martín, and J. Bonache, "On the radiation properties of split-ring resonators (SRRs) at the second resonance," *IEEE Trans. Microw. Theory Techn.*, vol. 63, no. 7, pp. 2133–2141, Jul. 2015.

[33] J. B. Pendry, A. J. Holden, D. J. Robbins, and W. J. Stewart, "Magnetism from conductors and enhanced nonlinear phenomena," *IEEE Trans. Microw. Theory Techn.*, vol. 47, no. 11, pp. 2075–2084, Nov. 1999.

[34] C. Reimann *et al.*, "Planar microwave sensor for theranostic therapy of organic tissue based on oval split ring resonators," *Sensors*, vol. 16, no. 9, p. 1450, 2016.

[35] R. K. Mongia, I. J. Bahl, P. Bhartia, and S. J. Hong, *RF and Microwave Coupled-Line Circuits*, 2rd ed. Boston, MA, USA: Artech House, 1999.

[36] J. Sor, Y. Qian, and T. Itoh, "Miniature low-loss CPW periodic structures for filter applications," *IEEE Trans. Microw. Theory Techn.*, vol. 49, no. 12, pp. 2336–2341, Dec. 2001.

JUN WANG was born in Jiangsu, China. He received the B.Eng. and M.S. degrees from Jiangsu Normal University, Xuzhou, China, in 2013 and 2017, respectively. He is currently pursuing the Ph.D. degree with Southeast University, Nanjing, China.

From 2015 to 2016, he was with the Department of Electronic and Electrical Engineering, Nanyang Technological University of Singapore, as a Research Associate. He has authored or co-authored over 10 referred journal and conference papers. His current research interests include the design of RF/microwave antennas and components.

LEI ZHAO (M'09–SM'18) received the B.S. degree in mathematics from Jiangsu Normal University, Xuzhou, China, in 1997, and the M.S. degree in computational mathematics and the Ph.D. degree in electromagnetic fields and microwave technology from Southeast University, Nanjing, China, in 2004 and 2007, respectively.

From 2009 to 2018, he was with the School of Mathematics and Statistics, Jiangsu Normal University. From 2007 to 2009, he was with the Department of Electronic Engineering, The Chinese University of Hong Kong, as a Research Associate. In 2011, he was with the Department of Electrical and Computer Engineering, National University of Singapore, as a Research Fellow. From 2016 to 2017, he was with the Department of Electrical and Computer Engineering, University of Illinois at Urbana–Champaign,Urbana, IL, USA, as a Visiting Scholar. He joined the China University of Mining and Technology, Xuzhou, China, in 2019, where he is currently a Full Professor. He has authored or co-authored over 50 referred journal and conference papers. His current research interests include antennas design and its applications, computational electromagnetics, electromagnetic radiation to human's body, and spoof surface plasmon polaritons design and its applications.

Dr. Zhao was a TPC member of many international conferences. He was the TPC Chair of the 2018 Cross Strait Quad-Regional Radio Science and Wireless Technology Conference. He serves as a Reviewer for multiple journals and conferences, including the IEEE Transactions on Antennas and Propagation, the IEEE Access, the IEEE Antennas and Wireless Propagation Letters, *Progress in Electromagnetics Research*, the ACES Journal, and other primary electromagnetics and microwave-related journals. He serves as an Associate Editor for the IEEE Access and an Associate Editor-in-Chief for the ACES Journal.

ZHANG-CHENG HAO (M'08–SM'15) received the B.S. degree in microwave engineering from Xidian University, Xi'an, China, in 1997, and the M.S. and Ph.D. degrees in radio engineering from Southeast University, Nanjing, China, in 2002 and 2006, respectively.

In 2006, he joined the Laboratory of Electronics and Systems for Telecommunications, École Nationale Supérieure des Télécommunications de Bretagne, Brest, France, as a Postdoctoral Researcher, where he was involved in the development of millimeter-wave antennas. In 2007, he joined the Department of Electrical, Electronic and Computer Engineering, Heriot-Watt University, Edinburgh, U.K., as a Research Associate, where he was involved in the development of multilayer integrated circuits and ultra-wideband components. In 2011, he joined the School of Information Science and Engineering, Southeast University, as a Professor. He has authored or co-authored over 150 referred journal and conference papers. He holds 20 granted patents. His current research interests include microwave and millimeter-wave systems, submillimeter-wave and terahertz components, and passive circuits, including filters, antenna arrays, couplers, and multiplexers.

Dr. Hao was a recipient of the Thousands of Young Talents presented by the China Government, in 2011, and the High Level Innovative and Entrepreneurial Talent presented by Jiangsu, China, in 2012. He has served as a reviewer for many technical journals, including the IEEE Transactions on Microwave Theory and Techniques, the IEEE Transactions on Antennas and Propagation, the IEEE Antennas and Wireless Propagation Letters, and the IEEE Microwave and Wireless Components Letters.